

Preparation, Characterization and Extraction Performance of Rubidium Ions in Water System of the Valinomycin-Functionalized Magnetic Solid-Phase Extraction Nanomaterial

Guo-jun Zhang, Hua Fu*, Hui-yuan Chen, Huo Liu, Wei-jun Song, Chun-yan Sun, Xin Hu and Yun Zhao**
School of Chemical Engineering, Qinghai University, 810016, Xining, PR China.
fuhua8711@126.com*, zhaoyun1003@163.com**

(Received on 29th October 2021, accepted in revised form 6th January 2022)

Summary: In this paper, a valinomycin-functionalized nano-sized magnetic solid-phase extractant (VFE) with the core-shell structure and the Fe₃O₄ nanospheres as the core is prepared. Related performances are characterized and tested by SEM, PPMS, XRD, FT-IR, TGA, EDS, ICP-MS, and AAS. The optimal extraction conditions are obtained, namely, temperature 50 °C or higher, *pH* not less than 9.3, and equilibrium extraction time about 35 min. Recycling performance experiments show that the extraction ratio of rubidium ions after 5 extraction-elution cycles is still up to 85.3%. Extraction experiments with the simulated brine, industrial wastewater, and domestic wastewater show that the VFE exhibits good selective extraction ability for rubidium ions in these water systems. This research is expected to provide a new method or a new material for the separation, extraction, enrichment, and detection of rubidium ions in water systems.

Key Words: Rubidium; Magnetic solid phase extraction; Nanomaterial; Valinomycin; Functional material.

Introduction

Rubidium has not only seen great progress in traditional applications such as electronic device, catalyst, special glass, biochemistry, and medicine, but also shown its application potential in high-tech fields such as magnetic fluid power generation, ion propulsion engine, and laser power converter [1]. It is a rare, precious and important strategic resource.

On the earth, large amounts of rubidium are stored in oceans and salt lakes. The rubidium reserved in seawater and salt lakes reaches about 1.9 billion tons and 10 million tons, respectively. Rubidium also exists in industrial wastewater, domestic wastewater and other water systems. However, rubidium concentrations in these water systems are all very low. For examples, the rubidium concentration is only 0.12 mg/L in seawater, 14 mg/L in the intercrystalline brine of Qarhan Salt Lake, and 60 mg/L in the Dead Sea brine. By contrast, the concentrations of K⁺, Ca²⁺, Na⁺, Mg²⁺ and other metal ions coexisting with Rb⁺ are much higher, and their physical and chemical properties also very similar to those of Rb⁺. The presence of these coexisting metal ions can seriously interfere with the extraction of rubidium from water systems [2-5].

Solid phase extraction

At present, the methods of extracting rubidium from water bodies can be roughly divided into two categories: precipitation method and extraction method.

For precipitation method, target metal ions in solution are reacted with the precipitation agent to generate insoluble compounds, and then the precipitated metal ions can be separated from the solution. It is mainly used to separate and extract rubidium from water bodies with high rubidium content.

For extraction method, in recent years, membrane extraction, ion imprinting extraction and solid phase extraction are also emerging as research hotspots in rubidium selective separation, besides traditional liquid phase extraction [6-11]. The membrane extraction mainly uses the polymer-based membrane as carrier, and functional molecules such as Benzo-18-Crown-6 or phosphomolybdic acid molecules are modified on the carrier, so as to selectively adsorb rubidium ions by the effect of size exclusion or ion exchange [12-14].

The ion imprinting extraction uses unsaturated small molecules as functional monomer, and rubidium ion as template, which is immobilized by a compound having the chelate effect. Then, the rubidium template ion, chelating agent and functional monomer are polymerized by an appropriate polymerization method. Finally, the rubidium template ions are removed and the imprinted cavities of rubidium ions can be left on the imprinting material, and the cavities can be used for selective extraction or adsorption of the rubidium ions [15-18].

*To whom all correspondence should be addressed.

The solid-phase extraction is to fix a functional molecule selective for rubidium ions onto a solid substrate by means of chemical synthesis [19-22]. It has many advantages. The individually targeted functional group can be modified, exhibiting higher selective extraction performance for target ions or compounds. Pretreatment operation process is simple, and can simultaneously achieve selective extraction, separation and enrichment for the target object, along with other advantages such as small amount of solvent required, short operation time, small sample dosage, and less interference. Therefore, the solid phase extraction has become a mainstream pretreatment method for complex system analysis [11]. It has already been broadly used in biology, medicine, and food industries for the separation, enrichment and detection of the organic substance or heavy metal ions in water systems in recent years [23, 24].

Magnetic solid phase extraction nanomaterial

The magnetic solid phase extraction technology has been extensively studied by scholars since it was proposed by Safarkov and Safark [24] in 1999. The magnetic extractant is superparamagnetic, and can be separated quickly from solution or suspension under an external magnetic field, which can replace traditional centrifugation, filtration or other operations [13, 14].

The magnetic nano-solid-phase extraction material combines the advantages of the magnetic solid-phase extraction material and nano-material. It has a large specific surface area that can be modified with a much larger amount of functional groups selective for the specific target ions, thus having a larger extraction capacity and higher selectivity [25, 26]. Such materials have been widely used in the extraction of rare and precious metal ions in low concentration solutions [26].

Research content and significance

The dimension of valinomycin cavity is similar to the diameter of hydrated rubidium ion [27]. Therefore, a valinomycin functionalized nano magnetic solid phase extractant (VFE) with the core-shell structure is prepared. Rubidium ions in solution can be selectively extracted by VFE based on the size sieving effect.

Performances of VFE are characterized, optimal extraction conditions and reusability are explored, and extraction abilities for the rubidium ions in complex water systems are researched.

It is expected to provide a novel material and a new idea for the separation, extraction, enrichment and

trace detection of the rubidium ions in oceans, salt lakes, industrial wastewaters, domestic wastewaters and other water bodies.

Experimental

General materials and instruments

The chemicals used in this study are purchased by different chemical suppliers, namely, Aladdin Industrial Company, Adamas Company, Tianjin Kaixin Chemical Industrial Co. Ltd, Yantai Shuangshuang Chemical Co. Ltd, Shanghai Haoran Reagent Co. Ltd, and Chengdu Jinshan Chemical Reagent Co. Ltd.

These chemicals include: $\text{FeCl}_3 \cdot 6\text{H}_2\text{O}$, trisodium citrate, ethylene glycol, anhydrous sodium acetate, ethanol, HCl solution, NH_3 aqueous solution, triethoxysilane, 3-aminopropyltriethoxysilane, methanol, acetic acid, glutaraldehyde, 1-(3-Dimethylaminopropyl)-3-ethylcarbodiimide hydrochloride (EDC), sodium cyanoborohydride, valinomycin, sodium cyanoborohydride, rubidium standard solution, HCl-Tris buffer solution, formic acid solution, sodium standard solution, potassium standard solution and magnesium standard solution.

The metal ions are determined using an atomic absorption spectrophotometer (AAS) Shimadzu AA6300C and an inductively coupled plasma mass spectrometer (ICP-MS) Thermo Fisher iCAP Qc. The particle size and morphology are studied by a scanning electron microscope (SEM) JEOL LTD JSM-6610LV. Spectra of energy dispersive spectroscopy (EDS) are obtained using an electron energy dispersive X-ray spectrometer JEOL LTD JEM-2100F. Fourier transforms infrared (FT-IR) spectra are obtained with a fourier transform infrared spectrometer US Perkin Eimer Company Spectrum BX-II. X-ray powder diffraction (XRD) patterns are recorded using a Bruker D8 FOCUS X-ray diffractometer. The magnetic measurements are carried out in a comprehensive physical property measurement system (PPMS) US Quantum Design Company PPMS-9T (EC-II). The thermo gravimetric analysis (TGA) is carried out on a simultaneous thermal analyzer Netzsch STA449F3. The solution *pH* values are adjusted using a Ohaus STARTER 3100 *pH* meter.

Preparation of $\text{Fe}_3\text{O}_4@ \text{SiO}_2$

Preparation of magnetic solid phase extraction agent generally includes the steps of magnetic core preparation and surface modification.

Scholars have explored many materials that

can be used as magnetic cores, such as ZnO, Fe₃O₄, nickel ferrite, Co₃O₄ and ZnFe₂O₄ [11, 23, 28]. Fe₃O₄ has been widely studied due to its simple preparation process and stable properties. In this paper, Fe₃O₄ is selected as the core material.

(1) Preparation of Fe₃O₄ nano magnetic core

A typical hydrothermal method is used to prepare the Fe₃O₄ nanospheres. The mixture of FeCl₃·6H₂O (1.36 g) and trisodium citrate (3.58 g) in ethylene glycol (70 mL) is stirred (speed 250 r/min) for 30 min at room temperature. Then anhydrous sodium acetate (7.09 g) is added. The mixture is stirred continuously for 30 min, which is then transferred to a 100 mL polytetrafluoroethylene reactor, and reacts in a vacuum oven at 200 °C for 10 h. In the end, Fe₃O₄ is separated by an external magnet, washed five times by ethanol and ultrapure water respectively, and then subject to vacuum drying overnight at 60 °C.

(2) Procedure for the synthesis of Fe₃O₄@SiO₂

The prepared Fe₃O₄ (0.15 g) is dispersed in HCl solution (50 mL, 0.1 mol/L) ultrasonically for 10 min. The attained Fe₃O₄ is also separated by an external magnet, and washed three times by ultrapure water and ethanol respectively. Then the washed Fe₃O₄ is dispersed in a mixture of ethanol and ultrapure water (80:20 mL) ultrasonically for 15 min. Then NH₃ aqueous solution (1 mL, 25%) and triethoxysilane (80 μL) are added in turn and drop-wise to the suspension. After continuous mechanical stirring vigorously for 12 h under nitrogen atmosphere at room temperature, the reaction is finished, and then the black product of Fe₃O₄@SiO₂ is collected and washed several times with ultrapure water and ethanol respectively, and finally dried overnight in vacuum condition at 60 °C.

Synthesis of VFE

After Fe₃O₄@SiO₂ is prepared, the coordination effect of oxygen is utilized to modify the surface of Fe₃O₄@SiO₂ with functional groups, which has a predetermined selectivity for the target ions.

(1) Synthesis of Fe₃O₄@SiO₂-NH₂

A particular NH₃ aqueous solution (5%) is added drop-wise to the mixture of ultrapure water (4.5 mL) and ethanol (36 mL) under stirring until pH=9.5, which is adjusted by a pH meter. Then 3-aminopropyltriethoxysilane (4.5 mL) is added drop-wise to the above suspension, and hydrolysis is performed under stirring for 4 h at room temperature. Then, Fe₃O₄@SiO₂ (1 g) is added to the resulting mixture and stirred at reflux under nitrogen atmosphere at 80 °C for 2 h. After reaction, the obtained Fe₃O₄@SiO₂-NH₂ is separated and washed several

times.

(2) General procedures for the synthesis of VFE

Solution A of methanol and acetic acid (1000:8 mL) is prepared.

The mixture of Fe₃O₄@SiO₂-NH₂, solution A (300 mL), glutaraldehyde (3 mL), and EDC (3.5 g) is stirred under nitrogen atmosphere at 40 °C and allowed to react for 10 h. Then, sodium cyanoborohydride (0.5 g) is added to the above solution, which continues to react for 2 h. After reaction, the attained black product is collected and washed ultrasonically several times with solution A.

Subsequently, the product is added to the mixture of solution A (300 mL), valinomycin (300 mg) and EDC (3.5 g), which react under nitrogen atmosphere at 40 °C for 10 h. Then, sodium cyanoborohydride (0.5 g) is added to the above suspension, which continues to react for 2 h. In the end, the black product of VFE is separated and washed ultrasonically several times with solution A, and dried overnight in vacuum condition at 60 °C.

Preparation process of VFE is shown in Scheme 1.

Optimum extraction conditions

(1) Extraction equilibrium time and kinetics

The VFE extractant (0.1 g) is added to a test tube containing rubidium standard solution (1 mL, 100 mg/L) and HCl-Tris buffer solution (9 mL, pH=9.5), and then the test tube is shaken by a shaker at constant temperature of 40 °C. With the development of extraction process, and under the different extraction time points, the concentrations of rubidium ions in the supernatants are detected by AAS. The extraction capacity is determined using the following equation (1):

$$Q_t = \frac{(C_0 - C_t)V}{m} \quad (1)$$

where Q_t (μg/g) is extraction capacity at time t ; C_0 and C_t (μg/mL) are rubidium ions concentration in supernatant at the initial time and t time respectively; V (mL) is the volume of supernatant, and m (g) is the mass of extractant.

An empirical exponential kinetic equation is used to describe the kinetics of the extraction process. The kinetic equation is:

$$v = kC_{Rb}^{\alpha} \quad (2)$$

where v ($\mu\text{g}/(\text{mL}\cdot\text{min})$) is the extraction rate, C_{Rb} ($\mu\text{g}/\text{mL}$) is the concentration of rubidium ions, k is the apparent extraction rate constant, and α is the observed extraction order.

Equation (2) can be modified to the form:

$$\lg v = \lg k + \alpha \lg C_{Rb} \quad (3)$$

From experimental data, the corresponding $\lg v$ - $\lg C_{Rb}$ curve can be obtained and values of α and k determined by slope and intercept, respectively [29].

(2) Optimal extraction pH value

The VFE extractant (0.1 g) is also added to a test tube containing rubidium standard solution (1 mL, 100 mg/L) and HCl-Tris buffer solution (9 mL), and then the test tube is shaken by a shaker at constant temperature of 40 °C for 35 min. Under different pH values, the concentrations of rubidium ions in the supernatants are detected by AAS, and the extraction capacity is also calculated with equation (1).

(3) Optimum extraction temperature

Similarly, the VFE (0.1 g) is added to a test tube containing rubidium standard solution (1 mL, 100 mg/L) and HCl-Tris buffer solution (9 mL, pH=9.5), and then test tube is shaken for 35 min. Under different temperatures, the concentrations of rubidium ions are detected by AAS, and corresponding extraction capacities are obtained.

Recycling performance of extractant

The VFE extractant (0.1 g) is added to a test tube containing rubidium standard solution (1 mL, 100 mg/L) and HCl-Tris buffer solution (9 mL, pH=9.5), and then the test tube is shaken at constant temperature of 50 °C for 35 min until the VFE is saturated with rubidium ions. Then, the saturated VFE is separated by an external magnet and washed several times with ultrapure water. After that, the rubidium ions are eluted from VFE by adding formic acid solution (10 mL, 1mol/L) three times. The concentrations of rubidium ions in the supernatants collected from each step above are detected by AAS. Herein, the elution ratio E (%) is calculated by equation (4):

$$E(\%) = \frac{W_D}{W_S} \times 100\% \quad (4)$$

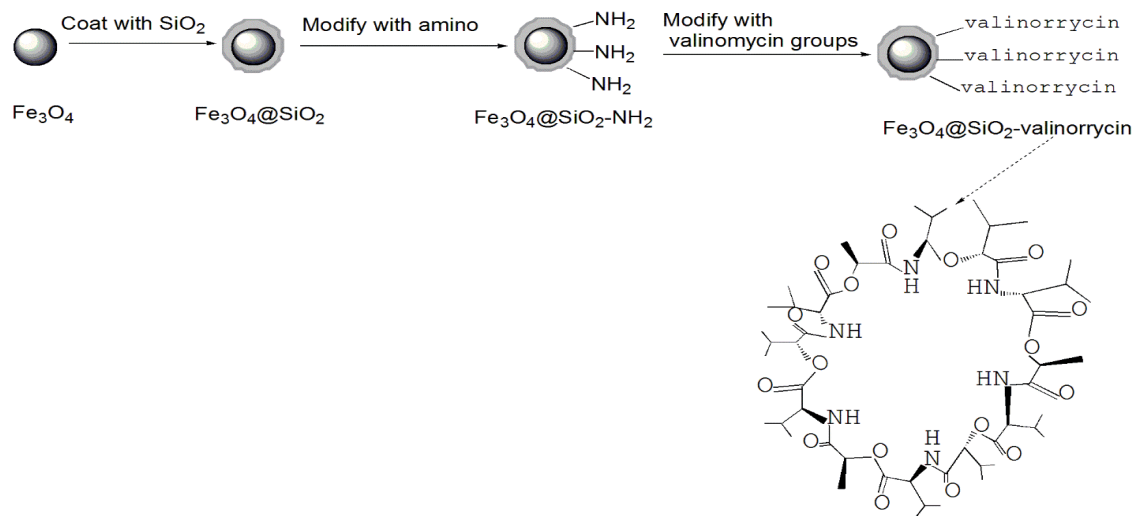
where W_D (μg) and W_S (μg) are the mass of eluted rubidium ions at each time and extracted rubidium ions at the first time, respectively.

This extraction-elution operation is successively performed 5 times to test recycling performance of this VFE extractant.

Extraction ratio Q (%) is calculated with the following equation (5):

$$Q(\%) = \frac{W_e}{W_S} \times 100\% \quad (5)$$

where W_e (μg) is the mass of extracted rubidium ions at each experiment.



Scheme-1: Schematic route of the preparation of VFE.

Extracting Rb⁺ from simulated brine

An artificial brine containing K⁺ (124.4 mg/L), Na⁺ (620.0 mg/L), Mg²⁺ (803.0 mg/L), Rb⁺ (50.0 mg/L) is prepared. The VFE extractant (50 mg) is added to a test tube containing the prepared simulated brine (1 mL) and HCl-Tris buffer solution (9 mL, *pH*=9.3), and then the test tube is shaken at constant temperature of 50 °C for 1 h. The concentrations of rubidium ions and other coexistence metal ions in the supernatant are detected by ICP-MS, and the extraction capacity is determined by equation (1).

Extracting Rb⁺ from industrial wastewater

VFE (30 mg) is activated by being dispersed in HCl-Tris buffer solution (1 mL, *pH*=9.3) ultrasonically for 10 min. Then the activated extractant is separated by an external magnet.

An industrial wastewater collected is neutralized to *pH*=7 by adding hydrous ammonia.

(1) Extraction process

The activated VFE is added to a test tube containing the neutralized industrial wastewater (500 µL), rubidium standard solution (500 µL, 13.7 µg/mL) and HCl-Tris buffer solution (1 mL, *pH*=9.3), and then the test tube is shaken using a vortex mixer at constant temperature of 50 °C. After extraction for 35 min, magnetic separation is performed, and saturated VFE is obtained, while the supernatant collected is transferred to a volumetric flask, and diluted with HCl-Tris buffer solution (*pH*=9.3) to 10 mL.

(2) Washing process

HCl-Tris buffer solution (500 µL, *pH*=9.3) is added to the saturated VFE and mixed thoroughly using a vortex mixer. Then magnetic separation is performed. This operation is repeated three times and then the supernatants are all transferred to one volumetric flask, and diluted with HCl-Tris buffer solution (*pH*=9.3) to 10 mL.

(3) Elution process

Formic acid (500 µL) is added to the washed saturated VFE, mixed thoroughly using a vortex mixer, eluting for 30min. Then magnetic separation is

performed. This elution operation is repeated two times. The supernatants are also all collected by one volumetric flask, and then diluted with HCl-Tris buffer solution (*pH*=9.3) to 10 mL.

ICP-MS is used to determine the concentrations of various metal ions in the diluted supernatants from the extraction, washing, and elution processes above.

Extracting Rb⁺ from domestic wastewater

Operation steps are the same as in the extraction experiments of industrial wastewater.

ICP-MS is also used to determine the concentrations of various metal ions in the diluted supernatants from each process.

Results and Discussion

Characterization

The SEM images of the magnetic core Fe₃O₄ and VFE particles are shown in Fig. 1a and Fig. 1b, respectively. According to the Figs, Fe₃O₄ particles are globular, monodispersed and of uniform size about 200 nm, and the appearance and size of VFE particles are roughly equivalent to those of Fe₃O₄.

The appropriate amount of silica added plays an important role in ensuring the proper specific surface area, particle size and magnetic strength.

From the results of SEM, the coated silica layer is relatively thin, and there is no excessive cross-linking during the reaction to cause particle aggregation. It suggests that the amount of silica added is appropriate.

PPMS results are shown in Fig. 2, where the magnetization curves show the saturation magnetization of Fe₃O₄ and VFE. As can be seen, both types of magnetic microspheres have superparamagnetism, and the magnetization is reduced to 56 A·m²·kg⁻¹ for VFE from 78 A·m²·kg⁻¹ for Fe₃O₄. The small difference is caused by the outer coating layer on the surface of the VFE microspheres. It confirms that the silica added does not have a great influence on the magnetic properties.

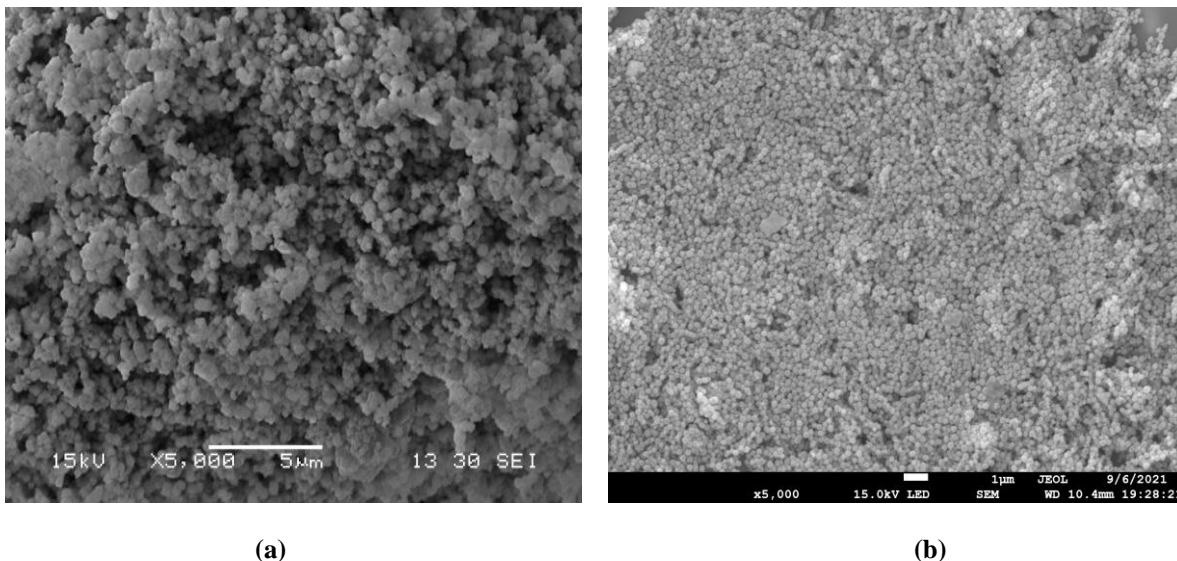


Fig. 1: SEM images of a) Fe_3O_4 and b) VFE (5000X magnification, under an acceleration voltage of 15 kV).

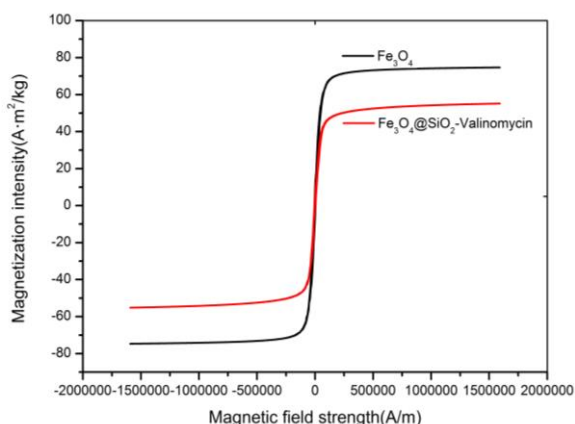


Fig. 2: Saturation magnetization curves of Fe_3O_4 and VFE (setting the initial magnetic field value to 0, at 300 K, and stabilizing for 30 minutes before test).

From the results of PPMS and SEM, the thickness of the coating layer of silicon dioxide is suitable.

As shown in Fig. 3, the VFE microspheres are able to be uniformly dispersed in water, and can also be quickly separated with water under an external magnetic field because of its superparamagnetism, which meets the requirement of convenient separation.

The FT-IR spectra of Fe_3O_4 , $\text{Fe}_3\text{O}_4@\text{SiO}_2$, and VFE are demonstrated in Fig. 4. The peaks observed at 578 cm^{-1} show the stretching vibrational modes of Fe-O are maintained in all samples. In Fig.

4b and 4c, the peaks of $\text{Fe}_3\text{O}_4@\text{SiO}_2$ and VFE near 805 cm^{-1} and 1093 cm^{-1} are attributed to the symmetric and asymmetric stretching vibrations of Si-O-Si. In Fig. 4c, the peaks at 3405 cm^{-1} , 1512 cm^{-1} and 1421 cm^{-1} are related to the stretching vibrations of amino group, C=O and isopropyl group of valinomycin, respectively. This indicates that the functional molecules of valinomycin has been successfully modified on $\text{Fe}_3\text{O}_4@\text{SiO}_2$ surface.

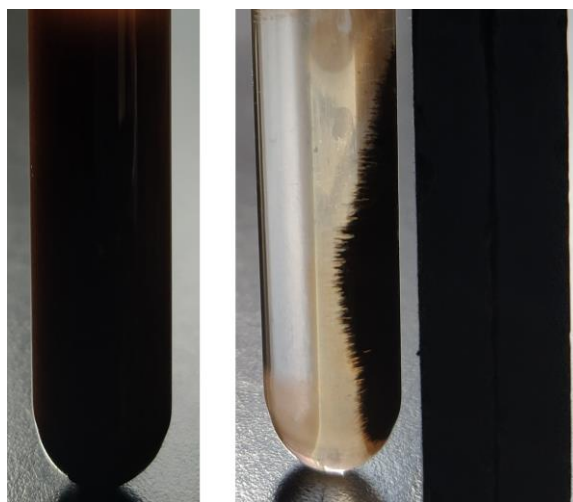


Fig. 3: Rapid separation of VFE under an external magnetic field (the left picture shows the phenomenon at the initial time, and the right picture shows the phenomenon at the 5 minutes after placing the magnet).

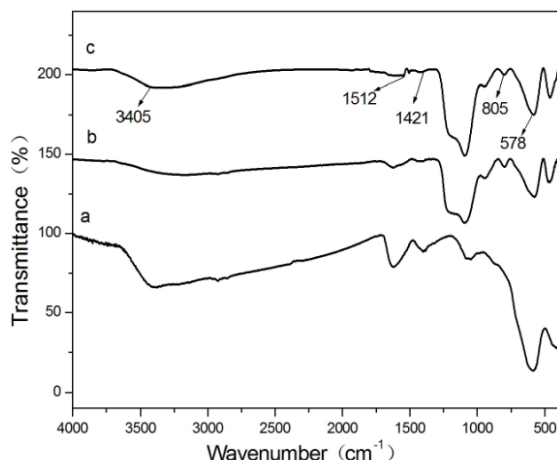


Fig. 4: The FT-IR spectra of a) Fe_3O_4 , b) $\text{Fe}_3\text{O}_4@ \text{SiO}_2$, and c) VFE (the sample weight is about 10mg, using KBr pellets).

Fig 5 shows the XRD patterns of Fe_3O_4 , $\text{Fe}_3\text{O}_4@ \text{SiO}_2$, and VFE.

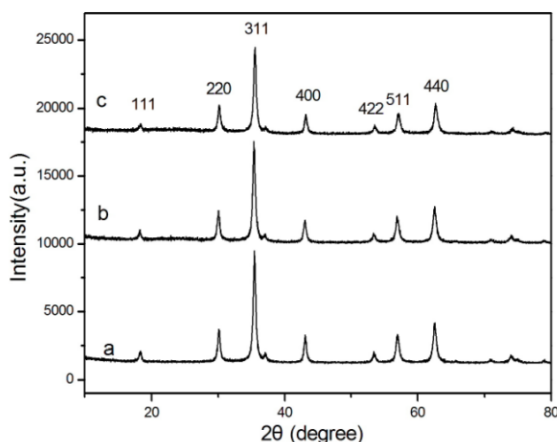


Fig. 5: The XRD patterns of a) Fe_3O_4 , b) $\text{Fe}_3\text{O}_4@ \text{SiO}_2$, and c) VFE (the measurement is made in 2θ ranging from 10° to 80° at the speed of $0.05^\circ \text{ min}^{-1}$, with Cu $K\alpha$ radiation).

The obvious peaks at $2\theta=17.98^\circ$, 30.02° , 35.46° , 42.98° , 53.39° , 57.03° and 63.6° belong to crystal diffraction of (111), (220), (311), (400), (422), (511) and (440) of Fe_3O_4 , and consistent with the standard XRD data of the structure of Fe_3O_4 . This indicates that the Fe_3O_4 substrate has not been damaged. The peak intensities of $\text{Fe}_3\text{O}_4@ \text{SiO}_2$ and VFE decrease slightly in the presence of SiO_2 and the SiO_2 -valinomycin coating-layer.

The thermal stability of the VFE sample is analyzed by TGA, as shown in Fig. 6. The weight loss between 40°C and 220°C may be caused by

water loss, while the weight loss between 220°C and 1200°C is because of thermal decomposition and skeleton collapse of valinomycin organic molecules. This demonstrates that VFE can exist stably below 200°C .

On the other hand, combining the results of infrared spectrum, it is confirmed that the amino group, valinomycin and other groups have been modified on the surface of the material. The weight loss is just because these organic groups are decomposed into small molecule gases.

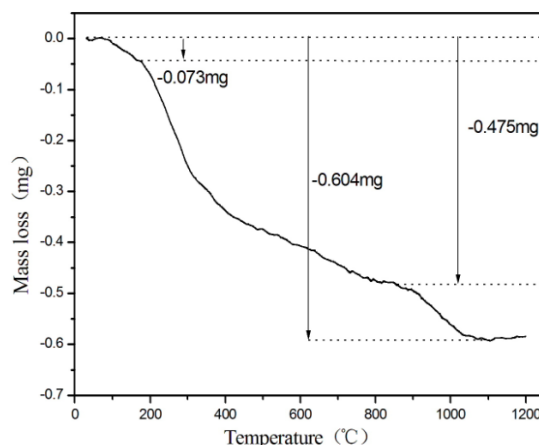


Fig. 6: TGA diagram of VFE (the sample amount is about 5 mg, and the heating rate is $5^\circ \text{C}/\text{min}$).

Fig 7 shows the EDS spectra of VFE before and after elution. It can be seen that the detected chief elements are O, Si, and Fe. They are derived from Fe_3O_4 , SiO_2 , and valinomycin. Herein, Cu is derived from the copper mesh used for testing. The Rb signal is detected as shown in Fig. 7a, and its mass percentage is 0.0922%, close to the equilibrium extraction amount, indicating that the extractant has successfully adsorbed the rubidium ions. On the other hand, no Rb signal is detected as shown in Fig. 7b, suggesting that the rubidium ions seem to have been eluted completely.

Optimal extraction conditions

(1) Effect of extraction time and kinetics

The experimental results at different extraction times are shown in Fig. 8. The extraction amount of rubidium ions gradually increases over time, and reaches the equilibrium saturation extraction amount of $924 \mu\text{g/g}$ at about 35 min.

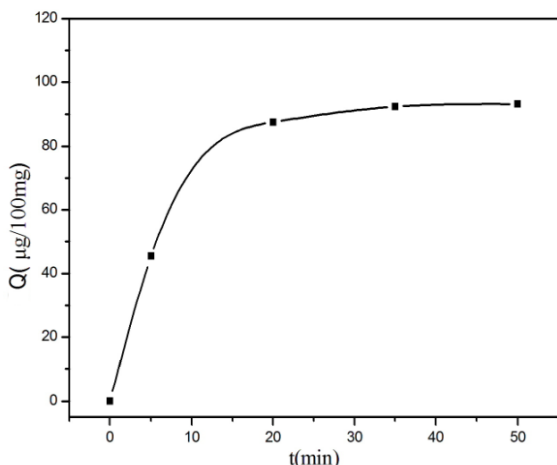


Fig. 8: Time-dependent rubidium extraction capacity of VFE (shaking at 9.5 pH and 40 °C, the concentrations of rubidium ions at each time point are detected by AAS).

The $\lg v$ - $\lg C_{Rb}$ line is presented in Fig. 9, and the correlation coefficient is 0.94. The values of the extraction order α and constant k are 1.72 and $0.0308 \mu\text{g}^{-0.72}/(\text{mL}^{-0.72} \cdot \text{min})$. Hence, an exponential kinetic equation is obtained:

$$v = 0.0308 C_{Rb}^{1.72} \quad (6)$$

(2) Effect of pH

The experimental results shown in Fig. 10 demonstrate that the equilibrium extraction capacity of VFE increases with increasing pH at the range of

8-9.3 and finally reaches the maximum value of 927 $\mu\text{g/g}$. Then the extraction capacity no longer increases with pH, and the optimal pH should be not less than 9.3.

(3) Effect of temperature

The experimental results shown in Fig. 11 reveal that the extraction capacity of VFE gradually increases with the rise of temperature at the range of 20-50 °C and the maximum value of 925 $\mu\text{g/g}$ is obtained under 50 °C or higher.

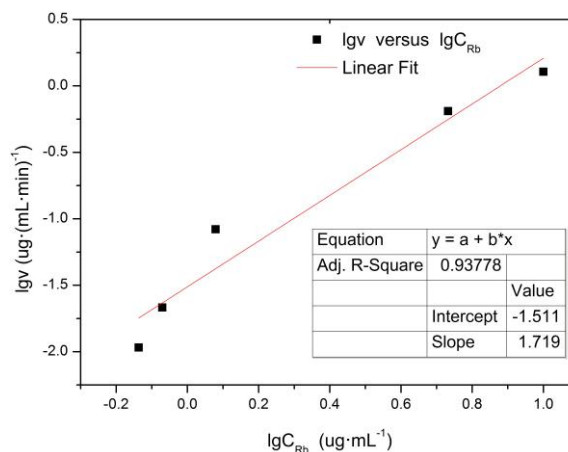


Fig. 9: The fitted straight line of $\lg v$ - $\lg C_{Rb}$ based on experimental data (at 40 °C).

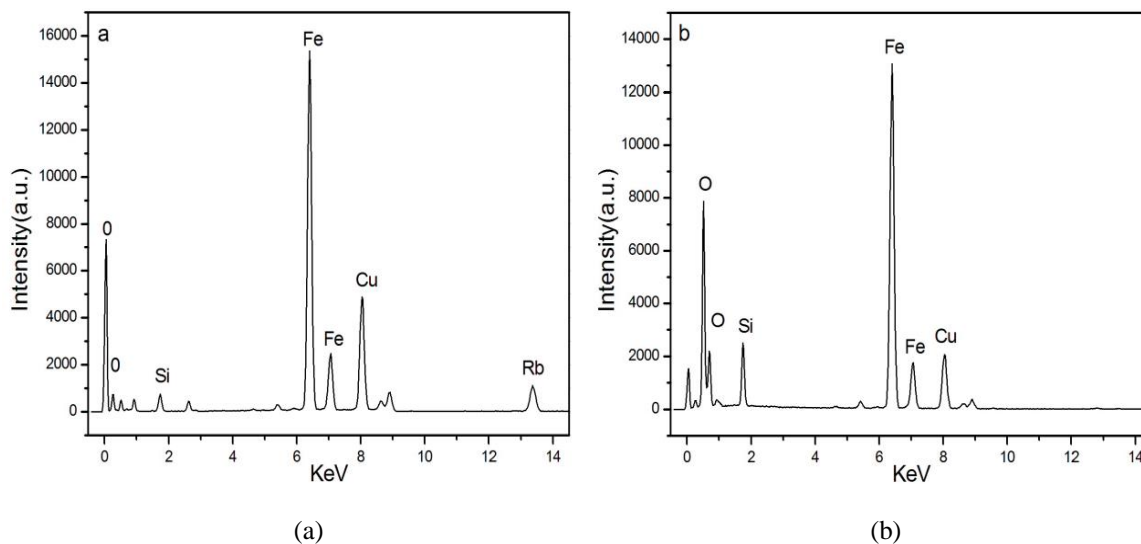


Fig. 7: EDS spectra of VFE a) before elution and b) after elution (under the voltage of 15 kV, WD 10 mm).

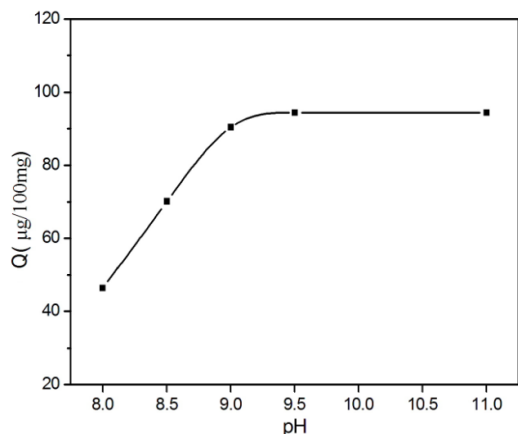


Fig. 10: *pH*-dependent rubidium extraction capacity of VFE (35 min shaking time at 40 °C, the concentrations of rubidium ions at each *pH* value are detected by AAS)

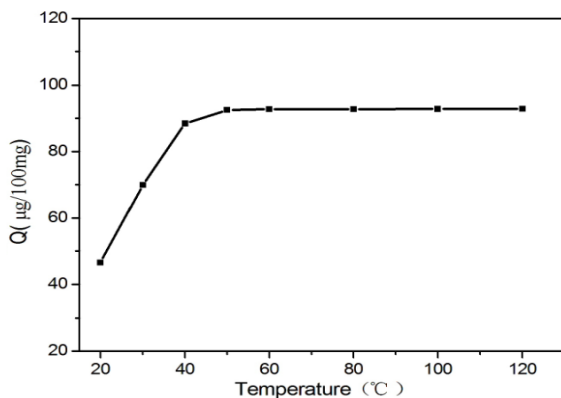


Fig. 11: Temperature-dependent rubidium extraction capacity of VFE (35 min shaking time at 9.5 *pH*, the concentrations of rubidium ions at each temperature point are detected by AAS).

A benzyl boryl functionalized extractant (BFE) was prepared in our previous research. The optimal rubidium extraction capacity of BFE was about 470 µg/g under the optimal extraction conditions and other experimental parameters were similar to those of VFE [30]. This demonstrates that rubidium extraction capacity of VFE is much better than that of BFE.

Reusability

The results of five successive extraction-elution experiments are shown in Fig. 12. The first elution ratio is 89.4%. After five extraction-elution cycles, the Rb⁺ extraction ratio of VFE still reaches 85.3%.

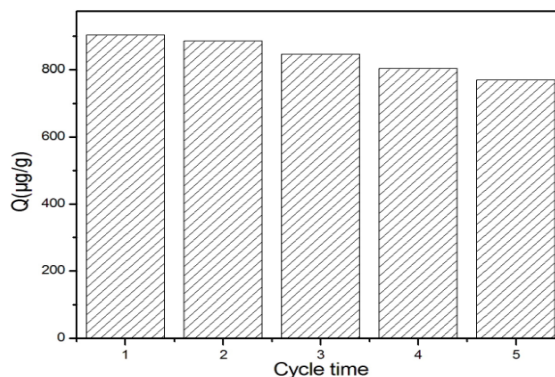


Fig. 12: Influence of the number of extraction cycles on extraction capacity of VFE (35 min extraction time at 9.5 *pH* and 50 °C for each cycle).

Simulated brine extraction experiment results

Fig. 13 shows the extraction amounts of various metal ions by VFE in simulated brine. The obtained extraction amounts of K⁺, Na⁺, Mg²⁺, and Rb⁺ are 62.3 µg/g, 85.3 µg/g, 139.5 µg/g, 891.2 µg/g, and the Rb⁺ extraction selectivity is 75.6%.

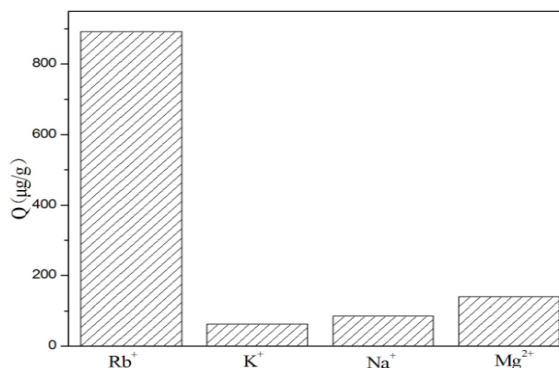


Fig. 13: VFE extraction capacity for Rb⁺ and coexistence ions in the simulated brine (1h extraction time at 9.3 *pH* and 50 °C, the concentrations of metal ions are detected by ICP-MS).

By comparison, at the same simulated brine, the extraction capacities of BFE for K⁺, Na⁺, Mg²⁺, and Rb⁺ were 3.2 µg/g, 93.3 µg/g, 113.2 µg/g, 348.3 µg/g, and the selectivity was 62.4% [30]. Thus VFE prepared in this paper has better rubidium extraction capacity and selectivity in simulated brine than BFE.

Industrial wastewater extraction experiment results

The data of various metal ions in different supernatants detected by ICP-MS is listed in Table-1.

The concentrations of Rb^+ in the supernatants after and before extraction are $30.8 \mu\text{g/L}$ and $687 \mu\text{g/L}$ respectively, and thus the apparent extraction ratio is about 95.5%. However, the Rb^+ concentration in the supernatant collected after elution is only $200 \mu\text{g/L}$, with a low recovery of 29%. The reasons may be as follows. First, the flocculent precipitate is observed during the process of neutralizing acidic industrial wastewater by hydrous ammonia, and this precipitate adsorbs some of the added rubidium ions; second, some added rubidium ions may be precipitated by reacting with some components of the very complex industrial wastewater system.

The extraction capacities of VFE for each metal ion in the industrial wastewater are shown in Fig. 14. As can be seen, the extractant has a strong selective extraction ability for rubidium ions in the industrial wastewater.

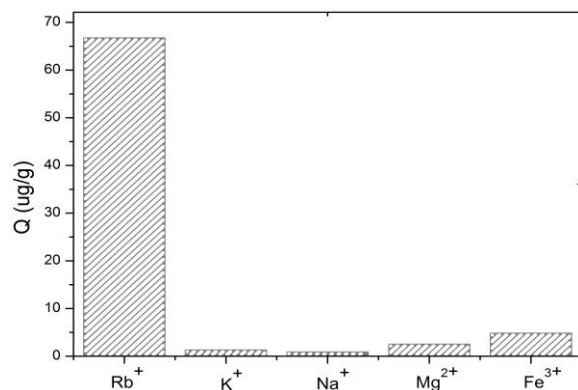


Fig. 14: VFE extraction capacity for various metal ions in the industrial wastewater (35 min extraction time at 9.3 pH and $50 \text{ }^\circ\text{C}$, the concentrations of metal ions are detected by ICP-MS).

Domestic wastewater extraction experiment results

As shown in Table 2, the concentrations of Rb^+ in the supernatants after and before extraction are $1.08 \mu\text{g/L}$ and $687 \mu\text{g/L}$ respectively, and thus the apparent Rb^+ extraction ratio is about 98.5%. Only a

small amount of rubidium ions is lost during the washing process, with a good recovery ratio of 83.8%.

The results shown in Fig. 15 demonstrate that the VFE has a stronger selectivity for the Rb^+ than other coexistence ions in the domestic wastewater.

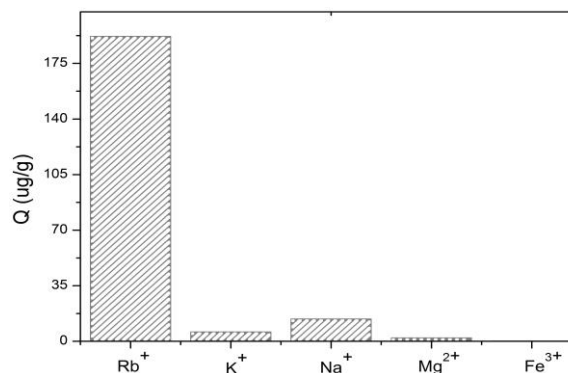


Fig. 15: VFE extraction capacity for metal ions in the domestic wastewater (35 min extraction time at 9.3 pH and $50 \text{ }^\circ\text{C}$, the concentrations of metal ions are detected by ICP-MS).

The material of VFE exhibits superparamagnetism and can be rapidly separated from a solution by introducing an external magnetic field, which can replace the traditional solid-liquid separation operations such as centrifugation and filtration.

In brief, this new Rb^+ extractant of VFE demonstrates the advantages of easy operation, quick separation, solvent saving, non-toxicity, good selectivity and reusability. Thus it is expected to provide a new method or material for the separation, extraction, enrichment, and detection of rubidium ions in some water systems.

Table-1: Extraction experiment results of the industrial wastewater.

Ions in diluted supernatants	Rb^+ ($\mu\text{g/L}$)	K^+ ($\mu\text{g/L}$)	Na^+ ($\mu\text{g/L}$)	Mg^{2+} ($\mu\text{g/L}$)	Fe^{3+} ($\mu\text{g/L}$)
Extraction process	30.8	14.7	88.7	3.27	1452
Washing process	-0.944	-0.217	6.78	0.874	91.7
Elution process	200	3.99	2.69	7.63	14.6

Table-2: Extraction experiment results of the domestic wastewater.

Ions in diluted supernatants	Rb^+ ($\mu\text{g/L}$)	K^+ ($\mu\text{g/L}$)	Na^+ ($\mu\text{g/L}$)	Mg^{2+} ($\mu\text{g/L}$)	Fe^{3+} ($\mu\text{g/L}$)
Extraction process	1.08	22.4	77.8	23.3	43.7
Washing process	6.68	1.15	26.2	0.874	7.36
Elution process	576	17.9	42.3	6.59	0.582

Conclusions

In this work, SiO₂ coated Fe₃O₄ was functionalized for the first time by valinomycin to prepare a novel extractant of VFE. Experimental results showed: the optimal extraction temperature is 50 °C or above, the *pH* value is not less than 9.3, and the equilibrium extraction time is about 35 minutes, and equilibrium extraction capacity for rubidium ions is about 927 µg/g. After five extraction-elution cycles, the extraction ratio for rubidium ions can still reach 85.3%.

Good selective extraction abilities of this extractant for rubidium ions in the simulated brine, industrial and domestic wastewater systems were demonstrated, suggesting that the VFE should be applied for Rb⁺ extraction in some actual samples containing coexistence ions at alkaline environment

Acknowledgements

The authors thank the financial support of the Natural Science Foundation of Qinghai Province (2019ZJ963Q).

References

1. L. Gao, G.H. Ma, Y.X. Zheng, Y. Tang, G.S. Xie, J.W. Yu, B.X. Liu and J.Y. Duan, Research trends on separation and extraction of rare alkali metal from salt lake brine: rubidium and cesium, *Solvent. Extr. Ion. Exc.*, **38**, 753 (2020).
2. X.F. Zhang, Z.F. Qin, T. Aldahri, S. Ren and W.Z. Liu, Solvent extraction of rubidium from a sulfate solution with high concentrations of rubidium and potassium using 4-tert-butyl-2-(alpha-methylbenzyl)-phenol, *J. Taiwan Inst. Chem. E.*, **116**, 43 (2020).
3. W. S. Chen, C.H. Lee, Y.F. Chung, K.W. Tien, Y.J. Chen and Y.A. Chen, Recovery of rubidium and cesium resources from brine of desalination through t-bambp extraction, *Metals.*, **10**, 607 (2020).
4. Z.H. Feng, L.Y. An, Z.G. Huang, X.Y. Zhao and B.G. Wang, Catalytic synthesis of 4-methyl-2-(alpha-methyl benzyl) phenol over Fe-Al-MCM-41 for extraction-separation rubidium from brine, *Rev. Roum. Chim.*, **65**, 141 (2020).
5. A.M. Bao and Z.Q. Qian, Study on solvent extraction behavior of rubidium by t-bambp-sulphonated kerosene system from salt lake brine, *J. Chem. Soc. Pakistan*, **41**, 1004 (2019).
6. Y.W. Lv, P. Xing, B.Z. Ma, Y.B. Liu, C.Y. Wang, W.J. Zhang and Y.Q. Chen, Efficient extraction of lithium and rubidium from polyolithionite via alkaline leaching combined with solvent extraction and precipitation, *ACS Sustain. Chem. Eng.*, **8**, 14462 (2020).
7. Y. Luo, Q.D. Chen and X.H. Shen, Complexation and extraction investigation of Rubidium ion by calixcrown-C(2)mimNTf(2) system, *Sep. Purif. Technol.*, **227**, 115704 (2019).
8. D.F. Huang, H. Zheng, Z.Y. Liu, A. Bao and B. Li, Extraction of rubidium and cesium from brine solutions using a room temperature ionic liquid system containing 18-crown-6, *Pol. J. Chem. Technol.*, **20** 40 (2018).
9. H.H. Tang, L.H. Zhao, W. Sun, Y.H. Hu, X.B. Ji, H.S. Han and Q.J. Guan, Extraction of rubidium from respirable sintering dust, *Hydrometallurgy*, **175**, 144 (2018).
10. Z.Li, Y. Pranolo, Z.W. Zhu and C.Y. Cheng, Solvent extraction of cesium and rubidium from brine solutions using 4-tert-butyl-2-(alpha-methylbenzyl)-phenol, *Hydrometallurgy*, **171**, 1 (2017).
11. S.M.Liu, H.H. Liu, Y.J. Huang and W.J. Yang, Solvent extraction of rubidium and cesium from salt lake brine with t-BAMBP-kerosene solution, *T. NONFERR. METAL. SOC.*, **25**, 329 (2015).
12. C. Yu, J. Lu, Z.Q. Hou, Z.F. Ma, X.Y. Lin, Z.Q. Dong, W.D. Xing, Y.S. Yan and Y.L. Wu, Mixed matrix membranes for rubidium-dependent recognition and separation: A synergistic recombination design based on electrostatic interactions, *Sep. Purif. Technol.*, **255**, 117727 (2021).
13. S.Q. Chen, X.X. Qin, W.X. Gu and X.S. Zhu, Speciation analysis of Mn(II)/Mn(VII) using Fe₃O₄@ionic liquids-beta-cyclodextrin polymer magnetic solid phase extraction coupled with ICP-OES, *Talanta*, **161**, 325 (2016).
14. Q. Wen, Y.Z. Wang, K.J. Xu, N. Li, H.M. Zhang and Q. Yang, A novel polymeric ionic liquid-coated magnetic multiwalled carbon nanotubes for the solid-phase extraction of Cu, Zn-superoxide dismutase, *ANAL. CHIM. ACTA*, **939**, 54 (2016).
15. Z.Y. Zhou, Y.L. Hu, Z. Wang, H.W. Zhang, B. Zhang and Z.Q. Ren, Facile preparation of a rubidium ion-imprinted polymer by bulk polymerization for highly efficient separation of rubidium ions from aqueous solution, *NEW. J. CHEM.*, **45**, 9582 (2021).
16. X.D. Zheng, Y.Y. Wang, F.X. Qiu, Z.Y. Li and Y.S. Yan, Dual-Functional Mesoporous Films Templated by Cellulose Nanocrystals for the

- Selective Adsorption of Lithium and Rubidium, *J. CHEM. ENG. DATA*, **64**, 926 (2019).
17. H.B. Li, Y.F. Qiao, J. Li, H.L. Fang, D.H. Fan and W. Wang, A sensitive and label-free photoelectrochemical aptasensor using Co-doped ZnO diluted magnetic semiconductor nanoparticles, *Biosens. Bioelectron.*, **77**, 378 (2016).
 18. C.Q. Wang, J. Qian, K. Wang, X.W. Yang, Q. Liu, N. Hao, C.K. Wang, X.Y. Dong and X.Y. Huang, Colorimetric aptasensing of ochratoxin A using Au@Fe₃O₄ nanoparticles as signal indicator and magnetic separator, *Biosens. Bioelectron.*, **77**, 1183 (2016).
 19. Z. Wang, A.Y. Zhang, J.T. Su and R.R. Chen, Selective adsorption of potassium and rubidium by metal-organic frameworks supported supramolecular materials, *J. Radioanal. Nucl. Ch.*, **329**, 359 (2021).
 20. Y.Z. Lyu, A.Y. Zhang and Y.N. Wang, Selective adsorption of rubidium onto a new 1,3-alternate calix[4]crown-5 mesoporous adsorbent with a polar carrier containing polyalkyl ester, *J. Chem. Eng. Data*, **65**, 198 (2020).
 21. T. Nur, P. Loganathan, M.A.H. Johir, J. Kandasamy and S. Vigneswaran, Removing rubidium using potassium cobalt hexacyanoferrate in the membrane adsorption hybrid system, *Sep. Purif. Technol.*, **191**, 286 (2018).
 22. I.U. Din, S. Tasleem, A. Naeem, M.S. Shaharun and Q. Nasir, Study of annealing conditions on particle size of nickel ferrite nanoparticles synthesized by wet chemical route, *Synth. React. Inorg. M.*, **46**, 405 (2016).
 23. B.S. Mohite and S.M. Khopkar, Solvent-extraction separation of rubidium with dicyclohexano-18-crown-6, *Talanta*, **32**, 565 (1985).
 24. M. Safarikova and I. Safarik., Magnetic solid-phase extraction, *J. Magn. Magn. Mater.*, **194**, 108 (1999).
 25. P. Xing, C.Y. Wang, Y.Q. Chen and B.Z. Ma, Rubidium extraction from mineral and brine resources: A review, *Hydrometallurgy*, **203**, 105644 (2021).
 26. D.J. Li, Y. Chen and Z. Liu, Boronate affinity materials for separation and molecular recognition: structure, properties and applications, *Chem. Soc. Rev.*, **44**, 8097 (2015).
 27. S. Ehala, J. Dybal, E. Makrlik and V. Kasicka, Capillary electrophoretic and computational study of the complexation of valinomycin with rubidium cation, *Electrophoresis*, **30**, 883 (2009).
 28. B. Ertan and Y. Erdogan, Separation of rubidium from boron containing clay wastes using solvent extraction, *Powder Technol.*, **295**, 254 (2016).
 29. Y. Zhao, S. S. Chen, S.H. Jin, L.J. Li, X.Y. Dong, R.T. Xing, Z.Y. Lu, Q.E. Liu, W. Li, and B. Zhang, Empirical Kinetics Equation of the Synthesis of NTO in Nitric Acid, *Propell. Explos. Pyrot.*, **41**, 1085 (2016).
 30. H. Liu, H. Fu, X.N. Wang, W.J. Song and C.Y. Sun, Synthesis and application of magnetic solid phase extractant functionalized by benzyl boryl, *Journal of Qinghai University*, **36**, 64 (2018).